Available online at www.eccomasproceedia.org
Eccomas Proceedia UNCECOMP (2025) 253-265

ECCOMAS
Proceedia

UNCECOMP 2025
6th ECCOMAS Thematic Conference on
Uncertainty Quantification in Computational Science and Engineering
M. Papadrakakis, V. Papadopoulos, G. Stefanou (eds.)
Rhodes Island, Greece, 15-18 June 2025

OPTIMAL SENSOR PLACEMENT FOR VIBRATION MONITORING OF BRIDGE STRUCTURES

Daniele Giunta[1], Eugenio Chioccarelli[1], Eleni Chatzi[2]

[1] Department of Civil Engineering, Energy, Environment and Materials, Università Mediterranea
Via Rodolfo Zehender - Feo di Vito, Reggio Calabria, 89124, Italy
{daniele.giunta, eugenio.chioccarelli}@unirc.it

[2] Department of Civil, Environmental, and Geomatic Engineering, ETH Zürich
Stefano-Franscini Platz 5, 8093, Zürich, Switzerland
chatzi@ibk.baug.ethz.ch

Abstract

A structural vibration-based monitoring system typically relies on deployment of a network of accelerometers on the monitored structure. Operational modal analysis tools are then commonly used for processing of the acquired data in order to extract the dynamic properties of interest. A crucial issue is to determine a sensor configuration that maximizes the accuracy in identification of the structural dynamic properties, while minimizing the required number of sensors and optimizing their locations. This task is commonly referred to as optimal sensor placement.

This study evaluates the performance of three methods for optimally selecting potential accelerometer locations based on their effectiveness in capturing the dynamic properties of the structure: the modal kinetic energy method, the effective independence method, and the information entropy method. These methods use results from modal analysis performed on a numerical model. To minimize the number of sensors, for each of the analyzed methods, an additional optimization step based on a modal frequency metric is adopted. This includes a numerical simulation of an ambient vibration test performed by exciting the finite element model of the structure with white Gaussian noise. The simulated acceleration responses are processed using the stochastic subspace identification with unweighted principal components technique.

The resulting procedures are applied to the case study of a prestressed concrete bridge, demonstrating that the optimized sensor network slightly depends on the adopted ranking method.

Keywords: Structural health monitoring, Operational modal analysis, Modal properties, Accelerometers, Optimization

Peer-review under responsibility of the organizing committee of UNCECOMP 2025.
doi: 10.7712/120225.12354.21227

1 INTRODUCTION

Structural health monitoring (SHM) has increasingly become essential for managing existing infrastructure, ensuring safety, reliability, and serviceability throughout their lifespan. An essential aspect of SHM is accurately assessing the dynamic behavior of structures through operational modal analysis (OMA), a methodology that extracts structural modal properties from measured vibration responses under operational conditions. A critical challenge in OMA relates to optimal sensor placement (OSP), which aims to strategically position sensors on a structure to maximize the accuracy of dynamic property identification. Different methodologies have been proposed in the literature for addressing the OSP problem. The modal kinetic energy (MKE) method [1], the effective independence (EFI) method [2] and the information entropy (IE) method [3] are among the most widely used methods [4,5]. All these OSP methods are based on the modal displacements derived from a numerical model of the studied structure, such as a finite element (FE) model. The MKE method prioritizes sensor locations where the structure exhibits maximum kinetic energy, thus enhancing signal quality for mode shape identification. The EFI method aims at maximizing the linear independence between the target mode shapes of the dynamic identification by ranking sensor positions based on their contributions to the Fisher information matrix. The IE method selects sensor positions to minimizing the uncertainty of structural parameters by means of entropy estimation.

Since all the OSP methods rank the candidate sensor locations but do not identify, by themselves, an optimal number (i.e., minimal number for the required accuracy) of sensors, a procedure to design a sensors network characterized by an optimized number and location of the sensors was discussed in previous works [6,7]. The procedure, that is identified hereafter as optimization of sensors network (OSN), was formulated coupling the ranking of sensor locations from the EFI method with a frequency metric, the cumulative frequency error (CFE), computed via a numerical simulation of the ambient vibration test of the monitored structure. Such a simulation was carried out through a linear dynamic analysis of the FE model. The simulated accelerations were then used to retrieve the modal frequency of the structure via a frequency domain decomposition (FDD) technique [8].

This work aims to extend the study of [6] by: (i) comparatively analyzing the performances of three different OSP methods, i.e., EFI, MKE, and IE, to be used for OSN; (ii) replacing the FDD technique with the stochastic subspace identification with unweighted principal components (SSI-UPC) technique [9] for the CFE computation.

In the following sections, the paper first provides a brief overview of the theoretical background of the considered OSP methods. Subsequently, the developed sensor network optimization algorithm, which is designed to efficiently determine the number of sensors based on frequency metrics, is detailed. Then, the case study structure, a prestressed concrete bridge, and its FE model are described. The results obtained from applying the optimization algorithm to the case study structure are presented, including a comparative analysis of the different OSP methods. Finally, the main findings of the research are summarized.

2 OPTIMAL SENSOR PLACEMENT METHODS

Among the different OSP techniques, the MKE, EFI, and IE methods were selected to evaluate the performance of the proposed optimization algorithm, as each uses distinct criteria to determine optimal sensor locations. The first step for implementing OSP methods is to create a FE model of the structure. Three input parameters are then defined: (i) a set of N target modes, obtained by performing a modal analysis of the model and representing the modes of interest for identification; (ii) a set of S candidate sensor locations on the structure; (iii) the number of sensors T to be deployed in the final configuration. The number of candidate locations S must exceed T, which in turn must be at least equal to N, as identifying a set of N modes requires at least $T = N$ sensors. All the sensors are considered as uniaxial accelerometers, meaning that each i-th sensor defines both its position and its measurement direction. This section outlines the analytical formulations of the considered OSP methods, while their typical workflow and how they are integrated into the proposed algorithm are presented in Section 3.

2.1 The modal kinetic energy method

The MKE method aims to enhance the modal information captured through sensor placement by positioning sensors where the kinetic energy contribution to the target modes is maximized. This sensor placement is expected to provide a higher signal-to-noise ratio and a more accurate mode shape identification [1,10]. The kinetic energy matrix $[MKE]$ is defined in Eq. (1):

$$[MKE] = [\Phi] \odot ([M] \cdot [\Phi]), \tag{1}$$

where $[\Phi]$ is the mode shape matrix of dimensions $[S \times N]$, containing the displacement of the i-th sensor ($i = 1, \dots S$) when the j-th mode ($j = 1, \dots N$) is activated, $[M]$ (dimensions $[S \times S]$) is the mass matrix that collects the values of the masses associated to each monitored node, $\odot$ denotes the element-wise product, and $\cdot$ the matrix product. Each element MKE_{ij} of the kinetic energy matrix is a scalar value that quantifies the contribution of the i-th sensor to the kinetic energy of the j-th mode. To assess the effectiveness of each sensor at maximizing the kinetic energy of all the target modes, MKE_i can be computed as per Eq. (2):

$$MKE_i = \sum_{j=1}^{N} MKE_{ij}. \tag{2}$$

The MKE_i is a ranking index for each sensor placement; higher values indicating more informative sensor positions for mode shapes identification.

2.2 The effective independence method

The EFI method is based on the computation of the Fisher Information Matrix $[FIM]$, which has dimensions $[N \times N]$ and is obtained as defined in Eq. (3):

$$[FIM] = [\Phi]^T [\Phi]. \tag{3}$$

The effective independence value, EFI_i, for the i-th sensor is defined as per Eq. (4):

$$EFI_i = \{\varphi\}_i \cdot [FIM]^{-1} \cdot \{\varphi\}_i^T, \tag{4}$$

where $\{\varphi\}_i$ is a row vector of dimensions $[1 \times N]$ containing the modal displacements of the i-th sensor for each of the N modes (i.e., the i-th row of the $[\Phi]$ matrix) and $[FIM]^{-1}$ is the inverse of the Fisher information matrix. The EFI_i index measures the contribution of the i-th sensor to the linear independence of the target mode shapes [2]. It ranges between 0 and 1, with higher values representing a greater contribution to modal identification.

2.3 The information entropy method

The IE approach measures the uncertainty associated with the system parameters $\{\theta\} \in \mathbb{R}^{N_\theta}$ in a Bayesian framework. In the OSP problem, the parameter vector $\{\theta\}$ may comprise the modal displacements (or other model parameters). N_θ is a scalar indicating the number of parameters to be estimated. The IE method aims to minimize the Shannon entropy of $\{\theta\}$, as lower entropy corresponds to reduced uncertainty in the system parameter estimation [3]. The information entropy IE for a given sensor configuration is defined in Eq. (5):

$$IE(\{\theta_0\}) = \frac{1}{2} N_\theta \ln(2\pi) - \frac{1}{2} \ln\left(\det([FIM(\{\theta_0\})])\right), \tag{5}$$

in which $\{\theta_0\}$ represents the optimal value of the parameter vector $\{\theta\}$ and the matrix $[FIM(\{\theta_0\})]$ is the Fisher information matrix with dimensions $[N_\theta \times N_\theta]$. For dynamic identification, which is the focus of this work, when the parameters $\{\theta\}$ correspond to the mode shapes, N_θ is set to N (i.e., the number of target modes), and the $[FIM]$ is computed as described in Eq. (3). Both the EFI method and the IEI method rely on the $[FIM]$ matrix since it is an indicator of the information contained in the data.

3 SENSOR NETWORK OPTIMIZATION ALGORITHM

This section outlines the proposed sensor network optimization algorithm. First, the traditional backward sequential sensor placement (BSSP) algorithm, which serves as the basis for the proposed approach, is described. Then, the OSP algorithm, defined to optimize sensor numbers using a frequency-based metric and including a numerical simulation of ambient vibration test, is presented.

3.1 The traditional OSP algorithm with BSSP

The OSP methods described in Section 2 can be implemented using a BSSP algorithm. In BSSP, the procedure begins by considering sensors deployed at all S candidate locations and removes one sensor per iteration. The sensor providing the least contribution to identifying the target modal parameters, based on the considered OSP method, is removed at each step. For the MKE and the EFI methods, the sensor to be removed is the sensor with the lowest value of the related index, i.e., the MKE_i and the EFI_i (see Eq. (2) and Eq. (4), respectively). For the IE method, the information entropy IE is computed as per Eq. (5) for the full set of S sensors. Rather than assigning a single-sensor index, the IE of all possible configuration subsets obtained by removing one sensor are evaluated, and the configuration with the lowest IE value is then retained and used to identify the sensor to be removed at each iteration. The iteration count is denoted as k. The procedure continues until the remaining sensors reach the desired number T, which occurs when $k = S - T + 1$. The general flowchart for this procedure is illustrated in Figure 1a.

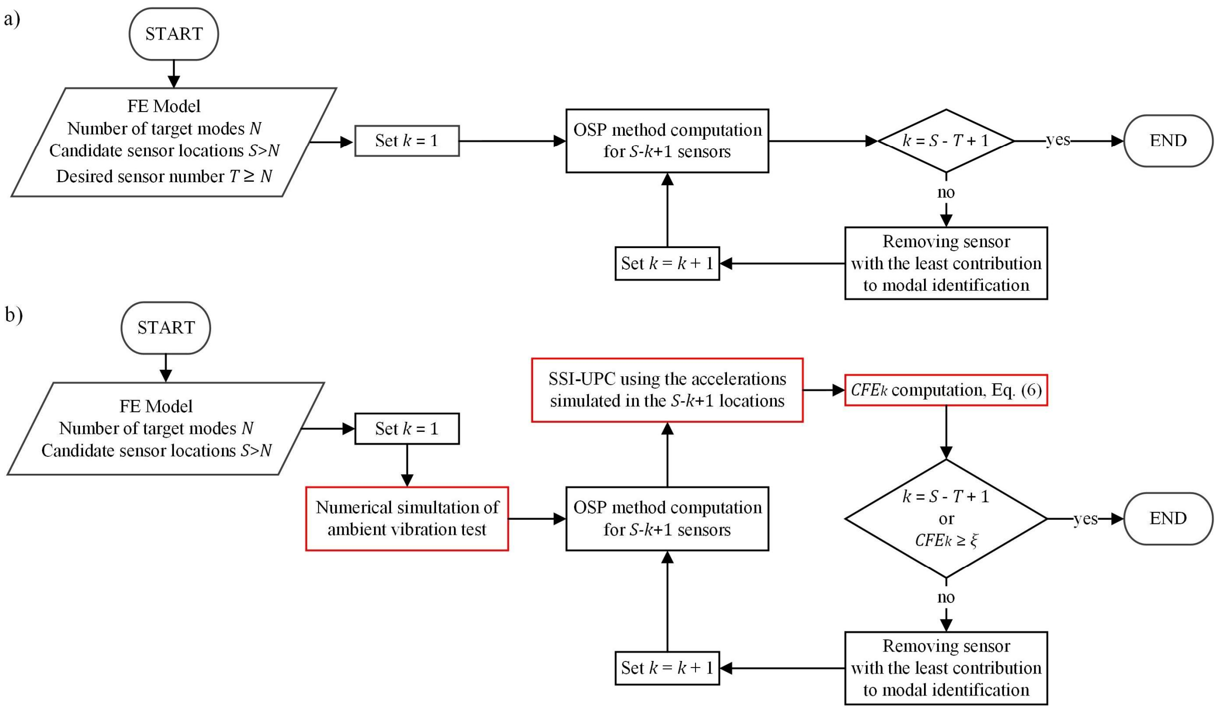

Figure 1. Flowcharts of OSP algorithms: (a) OSP methods using a BSSP algorithm (a); (b) OSN algorithm implementing numerical simulation of ambient vibration test.

3.2 The frequency-based OSN algorithm

The proposed algorithm integrates the outcomes from numerical modal analysis and operational modal analysis simulation based on the FE model. In Figure 1b, the flowchart of the algorithm is shown; red boxes highlight the steps introduced by this procedure compared to the BSSP procedure implemented for the traditional OSP methods. First, a FE model of the structure is realized and N target modes and S candidate sensor location are selected. Afterwards, a numerical simulation of ambient vibration test, employing white Gaussian noise as an excitation, is performed to replicate the vibration conditions expected during actual structural monitoring [11]. Such an excitation is applied along the three main directions at the base of the structure (exciting the whole model) and on the deck (emulating the random traffic excitation). From these simulations, acceleration time-histories at candidate sensor locations are generated. Then, the iterative procedure begins, setting the iteration count $k = 1$, and for each iteration of the algorithm, the effectiveness of each sensor location is assessed using an OSP method. Locations with lower rankings are iteratively excluded based on their limited contribution to the target modes identification.

The selection of an optimal sensor number is performed by introducing the CFE metric, quantifying differences between the numerically identified modal frequencies and the target frequencies from modal analysis [6,7]. The cumulative frequency error CFE_k, defined in Eq. (6), is computed as the sum of the relative difference between the frequency of the j-th mode identified by the numerical simulation, say $f_{DI,j}$, and the target frequency of the same mode, say $f_{FE,j}$ (obtained by the modal analysis of the FE model):

$$CFE_k = 100 \cdot \sum_{j=1}^{N} \frac{\left|f_{DI,j} - f_{FE,j}\right|}{f_{FE,j}}. \quad (6)$$

The iterative removal of sensor locations continues until CFE_k exceeds an acceptance threshold ξ or until the number of sensors equals the number of target modes N. Since factors such as monitoring system efficiency, identification objectives, number of target frequencies influence ξ, a case-specific approach should be considered for the definition of the threshold. Analyzing the variation of CFE_k with the sensor number can help to determine an appropriate threshold ξ (see Section 5).

In the previous application of this OSN algorithm discussed in [6], the FDD technique was used to retrieve the simulated modal frequencies. Herein, the simulated time series are analyzed using a subspace identification technique, the SSI-UPC technique. The SSI-UPC technique identifies the dynamic properties of structures by estimating a state-space model directly from the measured output data [12,13]. In contrast to frequency domain approaches, it operates entirely in the time domain. A key aspect of SSI-UPC is selecting an appropriate model order, representing the dimensions of the state-space model, which significantly influences the accuracy and reliability of the identified modal parameters [14]. The SSI-UPC was selected as identification technique due to its capability to estimate higher-frequency modes that were not identified using the peak-picking approach within the FDD. Capturing these higher-frequency modes is relevant, as they may manifest in dynamic identification of real structures, including the case-study structure discussed here. However, adopting SSI-UPC involves a trade-off in terms of computational time and effort. This issue is further discussed in Section 5.

As experimentally demonstrated in [6], the optimal sensor configuration identified by the presented OSN algorithm provides a sensor network capable of accurate natural frequency identification with the minimum number of required sensors.

4 CASE STUDY STRUCTURE AND FINITE ELEMENT MODEL

The selected structure is the Volto Santo Viaduct, a prestressed concrete bridge whose detailed geometry and actual monitoring data are reported in [6]. The side view of the bridge is presented in Figure 2 via a satellite picture. The bridge, located in Naples, Italy, consists of four 18.00 m simply supported decks supported by two abutments and three sets of circular-section reinforced concrete columns. Each span is composed of nine precast prestressed girders connected by crossbeams and topped with a cast-in-place reinforced concrete slab.

Figure 2. Satellite side view of the Volto Santo viaduct (satellite views © 2022 Google).

A three-dimensional FE model was set up using the FE software SAP2000 v24 [15] to represent one of the four typical spans of the viaduct, replicating the actual simply supported boundary conditions of the deck. The model discretizes the deck by combining frame elements for the girders and crossbeams, and shell elements for the reinforced concrete slab. The columns and bent caps are modeled via frame elements, with fixed supports at the base nodes. The model is shown in Figure 3.

The modal analysis of the FE model was performed to investigate the dynamic behavior of the structure and identify the target modes of interest for the OSN application. In Table 1 the modal frequencies and the description of the mode shapes are reported. The first five modes dominate the global response (e.g., the rigid translations of the deck, the vertical bending and torsion of the deck, and the global torsional mode). The remaining modes describe higher order bending and torsion of the deck.

The overall FE model captures both global and local modes of vibration that can be excited under ambient conditions. Thus, the model is used to: (i) compute the modal displacements that feed into the EFI, MKE, and IE methods; (ii) simulate the ambient vibration test with a linear dynamic analysis in order to generate acceleration time-histories for the CFE_k computation within the OSP procedure.

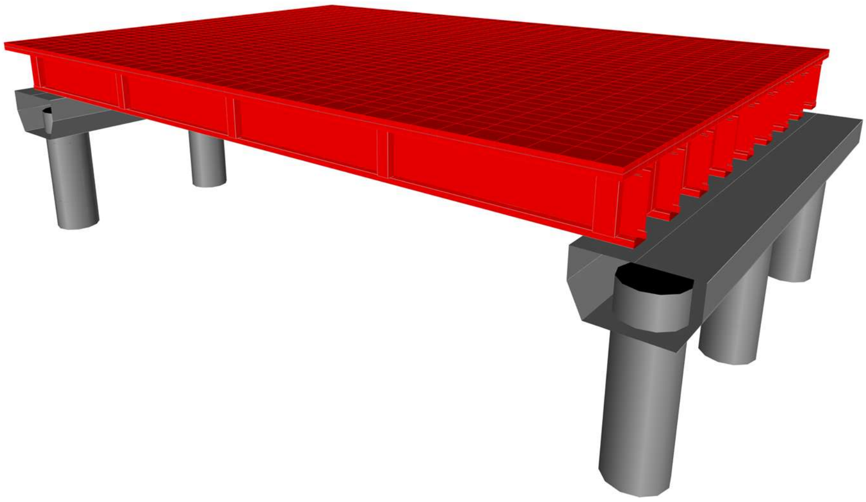

Figure 3. Tridimensional view of the FE model of the structure.

Table 1. Modal frequencies, f_{FE}, and description of the mode shapes obtained from the FE model.

Mode N.	f_{FE} (Hz)	Description
1	4.18	1st longitudinal translational global mode
2	6.15	1st vertical bending mode of the deck
3	6.90	1st torsional mode of the deck
4	6.79	1st transversal translational global mode
5	11.22	1st torsional global mode
6	15.92	2nd torsional mode of the deck
7	21.57	2nd vertical bending mode of the deck
8	21.85	3rd torsional mode of the deck
9	26.74	1st transversal bending mode of the deck
10	27.98	4th torsional mode of the deck

5 OPTIMIZED MONITORING SYSTEMS

To apply the OSN algorithm, $N = 9$ target modes were selected: modes 1 to 4 and 6 to 10 of Table 1. These modes were identified with a dynamic identification carried out on the actual structure. Mode 5 is neglected as it was not experimentally identified. It has to be noted that only the first four modes were selected as target modes in the previous application [6], as these were the only identifiable modes using the FDD technique. However, the adoption of the SSI-UPC technique in this work allowed the additional identification of the higher frequency modes, i.e., modes 6 to 10, thus, expanding the target mode number.

The candidate sensor locations were defined on the FE model, with a total of $S = 333$ sensors, corresponding to 111 nodes. At each node, it is considered that three uniaxial sensors are placed to capture the spatial acceleration of the monitored points. These nodes are distributed over the whole structure. In Figure 4 the axis of the columns and the beams composing the deck are sketched. The red dots are the selected nodes for the computation of the OSN procedure.

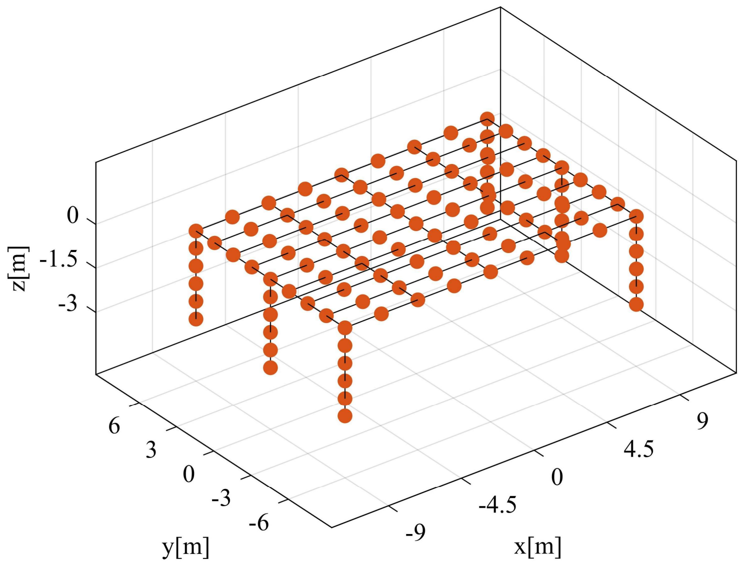

Figure 4. Candidate sensor locations defined on the FE model.

A linear dynamic analysis of the numerical model was performed by exciting the structure with white Gaussian noise. This analysis provided acceleration time series recorded at each candidate sensor with a sampling frequency of 100 Hz. The sampling frequency was chosen to ensure that the corresponding Nyquist frequency (50 Hz) exceeds the highest target frequency (Mode 10 – 27.98 Hz), allowing for accurate estimation of all modes up to the Nyquist limit. For each OSP technique (i.e., MKE, EFI, and IE), $(S - N + 1)$ sensor configurations were defined through the iterative procedure presented in Figure 1b, by sequentially removing sensor locations with the least contribution to modal identification based on the respective rankings (in the case of MKE, Eq. (1) was applied assuming the same mass value associated to each monitored node). As a result, a total of $3 \times (S - N + 1)$ sensor configurations were obtained. For each method and, thus, for each configuration, the cumulative frequency error CFE_k was computed. For this purpose, the time series were analyzed using the SSI-UPC technique implemented in the ARTeMIS Modal software [16]. The duration of the time series was 600 s, a sufficient duration for performing the considered identification technique. The SSI-UPC was performed for the first 32 sensor configurations obtained by the OSP rankings, i.e., with sensors ranging from 9 to 40 sensors. Thus, a total of 96 dynamic identifications were carried out. The lower bound (9 sensors) represents the minimum sensor number required to identify the 9 target modes, while the upper bound (40 sensors) was chosen as a reasonable limit to maintain feasibility in real applications of the OSN algorithm and to limit computational cost and processing time.

5.1 The SSI-UPC technique application within the OSP algorithm

This subsection discusses how model order selection influences the CFE estimation when applying the SSI-UPC technique for the numerical dynamic identification. The SSI-UPC dynamic identification was performed considering two different approaches: (i) for each considered sensor configuration, the model order providing the best solution in terms of frequency identification (with respect to the target modal frequencies) was selected; (ii) the order of the model used for frequency identification was fixed (set at a model order equal to 60 for this application, which was the maximum model order set in the first approach). Approach (i) aligns with the strategy commonly adopted in practical dynamic identification using subspace-based techniques [14]. Since the model order cannot be a-priori specified and should be at least twice the number of modes to be identified, an overestimation is typically introduced. As a result, spurious (i.e., numerical) modes appear in the model alongside the real modes. This overestimation often yields a more accurate estimation of the modes of interest. This approach introduces some randomness, as the model order selection remains partly arbitrary. On the other hand, approach (ii) removes this randomness by fixing the model order and speeds up the identification process. However, it may not always adapt well to changes in the measured data, thus potentially reducing the accuracy of frequency identification. Figure 5a and Figure 5b plot the CFE value as a function of the sensor number for the two approaches, using different colors and markers for each OSP method. In approach (i) (see Figure 5a), for all the considered OSP methods, the CFE has a clear trend, as it starts at approximately 25% for 9-sensor configurations, decreases to about 15% up to 23 sensors, and remains constant as the sensor number further increases. Beyond 24 sensors, MKE configurations fail to identify mode 1 frequency (translational longitudinal mode) due to excessive presence of sensors in the vertical direction, reducing sensitivity to this horizontal mode. This limitation is indicated in the plot with grey markers for MKE configurations unable to estimate the frequency of mode 1. In Figure 5b, related to approach (ii), the obtained CFE does not show a clear trend increasing the sensor number. This behavior suggests that increasing the number of monitored degrees of freedom, without adjusting the identification parameters, does not always lead to a significant improvement in frequency identification accuracy. Instead, with approach (i), the adaptive nature of the method effectively uses additional data, gradually reducing uncertainty. However, once a stable information level is reached, adding more sensors no longer provides meaningful additional insights. These results conceptually align with findings in [17], discussing that classical Bayesian model updating cannot explicitly quantify modeling errors, since these are lumped together with other sources of uncertainty such as measurement noise and parameter variability. As a result, if modeling errors are significant, additional data might not provide meaningful new insights unless these errors are separately characterized and accounted for. Although the presented application is focused on OSN rather than Bayesian updating, a similar effect is observed: simply increasing the sensor number (monitored degrees of freedom) without adapting identification parameters (such as model order) does not always lead to improved frequency estimation accuracy. This aspect highlights how adjusting identification parameters (approach (i)) benefits frequency estimation in this OSN application, as shown by the CFE trends in Figure 5a and Figure 5b. Thus, the remaining part of this application will refer to Figure 5a.

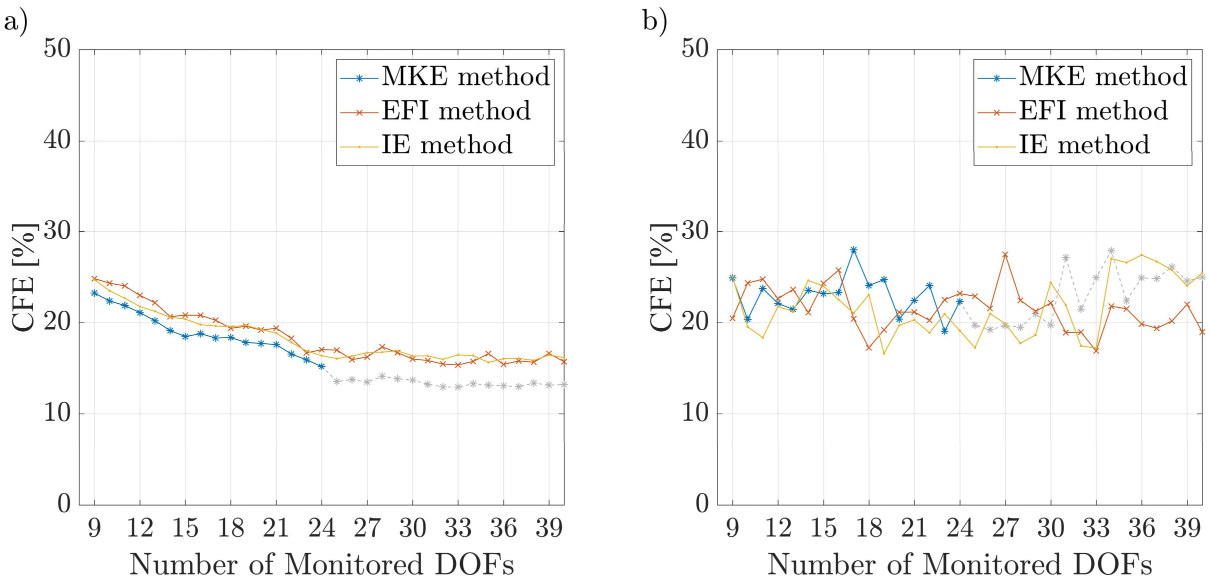

Figure 5. Cumulative frequency error varying the number of sensors: (a) adaptive model order selection – approach (i); (b) fixed model order – approach (ii).

5.2 OSP methods comparison

Figure 5a shows that all three OSP methods exhibit similar trends in CFE, as they distribute sensors in a comparable manner as the number of monitored degrees of freedom increases. In addition to the previously mentioned variations in slope at 9 and 23 sensor configurations, another significant feature of the plot in Figure 5a occurs at 15 sensors, where a reduction in the slope of the curves can be observed. In Figure 6a, Figure 6b, and Figure 6c, the 15-sensor configurations for the MKE, the EFI, and the IE methods are shown, respectively. In each figure, arrows indicate sensors measuring along the horizontal directions and dots denote sensors recording along the vertical direction. As depicted, although the sensor placement carried out with the three methods is similar, distributing sensors along the deck, the MKE method places only vertical sensors as it tends to maximize the kinetic energy of the considered modes. Since 6 out of 9 target modes are vertical modes of the deck, the method places sensors in the vertical direction at nodes where modal displacements are largest. Hence, sensor configurations with a low number of monitored degrees of freedom obtained using the MKE method are not able to properly capture the mode shapes of horizontal modes, such as Mode 1, Mode 4, and Mode 8 described in Table 1, as no sensors are placed along the horizontal directions. However, mode shape reconstruction was not taken into account in the OSN procedure, as the optimization was performed considering the target modal frequencies as objective through the CFE metric. As suggested in [4,5], trade-offs between different OSP metrics should be considered in an optimization procedure, e.g., including a metric based on the mode shape comparison. Nevertheless, frequency identification of these modes was still achieved using the sensor configurations derived from the MKE method, allowing to compare the results in terms of CFE between this method and the EFI and IE methods. On the other hand, the EFI and IE methods prioritize maximizing the independence and information content of all the target mode shapes. As a result, they tend to distribute sensors ensuring that all mode shapes can be captured. Such configurations allow the reconstruction of all the nine target mode shapes.

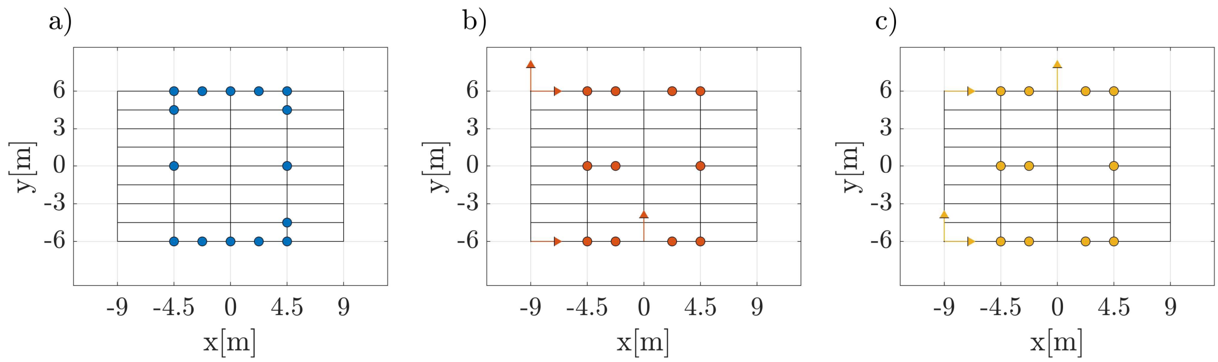

Figure 6. 15-sensor configuration obtained by using (a) the MKE, (b) the EFI and (c) the IE methods.

The optimal configurations (i.e., those minimizing the CFE value and allowing the target frequency identification) should be selected at 33 sensors (CFE = 15.38%) for the EFI method, 35 sensors (CFE = 15.65%) for the IE method, and 24 sensors (CFE = 15.19%) for the MKE method. However, all methods converge to comparable CFE values once the sensor number reaches about 23-24. Thus, selecting 23-sensor configuration as optimal can be considered a reasonable compromise for this application. Figure 7 illustrates the resulting optimal sensor configurations obtained using the three OSP methods, showing that while orientation preferences differ, the final configurations are similar and provide analogous frequency identification accuracy.

This comparative study extends the optimization approach introduced in [6], by verifying that the CFE metric remains robust across different OSP methods and by introducing the SSI-UPC technique as a valuable tool for extracting modal frequencies within the numerical dynamic identification process. The experimental validation of the applied OSN algorithm was already discussed in [6].

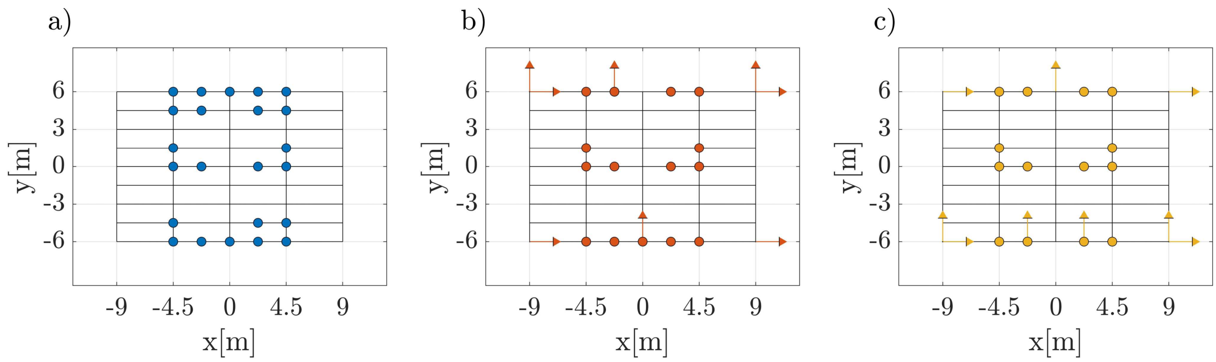

Figure 7. Optimal sensor configurations for different OSP methods: (a) MKE; (b) EFI; (c) IE.

6 CONCLUSIONS

In this study, three well-known OSP methods, i.e., the MKE, the EFI, and the IE methods, were compared using an optimization algorithm based on the CFE metric to an existing bridge. This work extends previous investigations by implementing a subspace identification technique, the SSI-UPC technique, within the OSN algorithm, providing a more robust and reliable assessment of the modal frequencies. The main findings of this work can be summarized as follows:

- All three OSP methods achieved similar sensor configurations and converged to comparable CFE values for the selected target modes. While the MKE method tends to place sensors in the vertical direction (reflecting the dominance of vertical modes), the EFI and IE methods distribute sensors more evenly across both horizontal and vertical directions.

- The adoption of the SSI-UPC identification technique improved frequency identification accuracy compared to the frequency-domain identification method used in a previous study. This improvement allowed for an increased number of target modes as input of the OSN algorithm, matching the number of actual modes identified through an OMA conducted on the real case study structure. However, the reliance on numerical modeling and computational resources represents a limitation.
- Across all methods, the CFE stabilized around a sensor number of 23–24, indicating that beyond this number, additional sensors contributed minimal improvements to frequency identification. Hence, 23 sensors emerged as a reasonable compromise between accuracy and feasibility.

In conclusion, while numerical simulations and computational demands remain a practical limitation, the results highlight the robustness of the CFE-based OSN algorithm.

7 ACKNOWLEDGEMENTS

The presented work has been partially supported by the project “DS2: Digital Smart Structures”, funded by INAIL (Italian Workers’ Compensation Authority), BRIC 2021 and partially carried out as part of the activities envisaged by the Agreement between the High Council of Public Works (CSLLPP) and the ReLUIS Consortium implementing Ministerial Decree 578/2020 and Ministerial Decree 240/2022. Prof. Chatzi wishes to acknowledge the MSCA Staff Exchanges 2021 project ReCharged (Grant ID: 101086413). This project has received funding from the Horizon Europe Programme under the Marie Skłodowska-Curie Staff Exchanges Action (GA no. 101086413), co-funded by the UK Research & Innovation and the Swiss State Secretariat for Education, Research & Innovation. The contents of this paper represent the authors’ ideas and do not necessarily correspond to the official opinion and policies of the funding entities.

REFERENCES

[1] G. Heo, M.L. Wang, D. Satpathi, Optimal transducer placement for health monitoring of long span bridge. *Soil Dynamics and Earthquake Engineering*, **16**, 495–502, 1997. https://doi.org/10.1016/S0267-7261(97)00010-9.

[2] D.C. Kammer, Sensor placement for on-orbit modal identification and correlation of large space structures. *Journal of Guidance, Control, and Dynamics,* **14**, 251–259, 1991. https://doi.org/10.2514/3.20635.

[3] C. Papadimitriou, Optimal sensor placement methodology for parametric identification of structural systems. *Journal of Sound and Vibration,* **278**, 923–947, 2004. https://doi.org/10.1016/j.jsv.2003.10.063.

[4] C. Leyder, V. Dertimanis, A. Frangi, E. Chatzi, G. Lombaert, Optimal sensor placement methods and metrics–comparison and implementation on a timber frame structure. *Structure and Infrastructure Engineering,* **14**, 997–1010, 2018. https://doi.org/10.1080/15732479.2018.1438483.

[5] M. Meo, G. Zumpano, On the optimal sensor placement techniques for a bridge structure. *Engineering Structures,* **27**, 1488–1497, 2005. https://doi.org/10.1016/j.engstruct.2005.03.015.

[6] E. Chioccarelli, D. Giunta, A. De Angelis, A. Bilotta, Discussing optimal sensor placement for ambient vibration test of an existing bridge. *Engineering Structures,* **310**, 2024. https://doi.org/10.1016/j.engstruct.2024.118000.

[7] P. Pachón, M. Infantes, M. Cámara, V. Compán, E. García-Macías, M.I. Friswell, R. Castro-Triguero, Evaluation of optimal sensor placement algorithms for the Structural Health Monitoring of architectural heritage. Application to the Monastery of San Jerónimo de Buenavista (Seville, Spain). *Engineering Structures*, **202**, 2020. https://doi.org/10.1016/j.engstruct.2019.109843.

[8] R. Brinker, L. Zhang, P. Anderson, Modal identification of output-only systems using frequency domain decomposition. *Smart Materials and Structures*, **10**, 2001. https://doi.org/10.1088/0964-1726/10/3/303.

[9] P. Van Overschee, B. De Moor, *Subspace identification for linear systems*, Springer US, 1996. https://doi.org/10.1007/978-1-4613-0465-4.

[10] M. Papadopoulos, E. Garcia. Sensor placement methodologies for dynamic testing. *AIAA Journal*, **36**, 256–263, 1998. https://doi.org/10.2514/2.7509.

[11] V. Pepe, A. De Angelis, M.R. Pecce, Numerical simulation of ambient vibration tests: A case study. *7th International Conference on Advances in Experimental Structural Engineering,* EUCENTRE, Pavia, Italy, 2017. https://doi.org/10.7414/7aese.T5.200.

[12] R. Brinker, C. Ventura, *Introduction to Operational Modal Analysis*. John Wiley & Sons, Ltd, 2015. https://doi.org/10.1002/9781118535141.

[13] K.S. Arun, S.Y. Kung, Balanced approximation of stochastic systems. *SIAM Journal on Matrix Analysis and Applications*, **11**, 807–819, 1990. https://doi.org/10.1137/0611003.

[14] C. Rainieri, G. Fabbrocino, *Operational modal analysis of civil engineering structures: An Introduction and Guide for Applications*. Springer, 2014. https://doi.org/10.1007/978-1-4939-0767-0.

[15] Computers & Structures inc., Structural and earthquake engineering software. SAP2000 Version 24, (2016).

[16] Structural Vibration Solutions A/S. ARTeMIS Modal Pro Version 6.0, (2019).

[17] M. Song, I. Behmanesh, B. Moaveni, C. Papadimitriou, Modeling error estimation and response prediction of a 10-story building model through a hierarchical bayesian model updating framework. *Frontiers in Built Environment*, **5**, 2019. https://doi.org/10.3389/fbuil.2019.00007.